

# 플란지 평행도파관에 의한 산란 및 수신 : TE-모드 해석 (Scattering and Reception by a Flanged Parallel-Plate Waveguide : TE-Mode Analysis)

박 타 준\* , 엄 효 준\*  
(Tah J. Park, Hyo J. Eom)

## ABSTRACT

The TE-mode characteristics of scattering and reception by a flanged parallel-plate waveguide are examined. The technique of the Fourier transform is used to represent the scattered fields in the spectral domain. The simultaneous equations for the transmitted field coefficients are solved to obtain the solution in an asymptotic series form. The numerical computations are performed to illustrate the behaviors of the scattered field and the transmission coefficients versus the aperture size.

## 요 약

플란지 평행도파관에 의한 TE-모드의 산란 및 수신을 해석한다. 푸리에 변환을 이용하여 주파수 영역에서 산란파를 표시하여, 경계조건을 사용하여 산란파의 점근해를 구하였다. 수치해석을 통하여 산란특성을 조사하였다.

## I. Introduction

Electromagnetic scattering from a conducting double-wedge has been extensively studied with the asymptotic high-frequency techniques [1,2] since the exact solution in a closed form is still unknown. TM-mode scattering from a flanged parallel-plate waveguide (a special double-wedge geometry) was considered in [3] using the Weber Schafheitlin integral technique. In this paper, we

examine the TE-mode scattering from the flanged waveguide by utilizing the Fourier transform and the mode-matching technique [4,5]. In the next Section, we present the scattered field in asymptotic series which simplify to a closed form in the high frequency limit. Numerical computations are performed in Section 3 to illustrate the behavior of the scattered field and the transmission coefficient. A brief summary on the theoretical development is given in Concluding Remarks.

\*한국과학기술원 전기공학과

\*Department of Electrical Engineering Korea Advanced Institute of Science and Technology

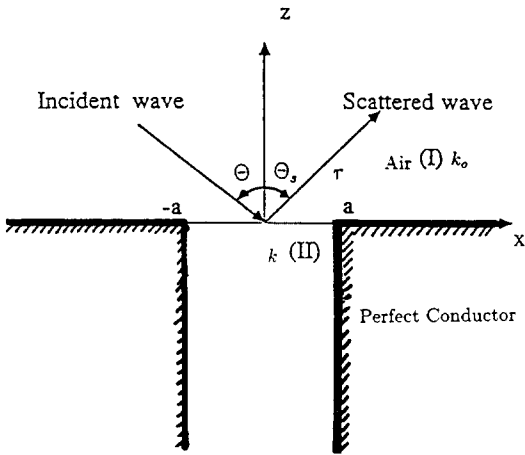


Fig. 1. Scattering Geometry

## II. Scattered and Received Fields Derivation

Fig. 1 shows a perfect-conducting flanged parallel plate waveguide of width  $2a$ . In Region (I) ( $z > 0$ ), an incident field  $E_y^i$  (TE mode: transverse-electric-to-propagation-direction) impinges on the flanged parallel-plate waveguide. Region (II) ( $z < 0, -a < x < a$ ) denotes the waveguide interior. The wave numbers of Regions (I) and (II) are  $k_0$  ( $= 2\pi/\lambda$ ) and  $k$ , respectively and  $e^{-j\omega t}$  time factor is suppressed.

Then in Region (I), the total electric field consists of the incident, reflected, and scattered fields which are respectively written as

$$E_y^i(x, z) = e^{jk_x x - jk_z z}$$

$$E_y^r(x, z) = -e^{jk_x x + jk_z z}$$

$$E_y^s(x, z) = 1/(2\pi) \int_{-\infty}^{\infty} \bar{E}_y^s(\zeta) e^{j\zeta x + jk_z z} d\zeta$$

$$\text{where } k_x = k_0 \sin\theta$$

$$k_z = k_0 \cos\theta$$

$$k_1 = \sqrt{k_0^2 - \zeta^2}$$

$$\bar{E}_y^s(\zeta) = \int_{-\infty}^{\infty} E_y^s(x, 0) e^{j\zeta x} dx$$

Since  $H_x(x, z) = -1/(j\omega\mu) \partial E_y(x, z) / \partial z$ , the corresponding  $x$  components of the incident, reflected, and scattered H-fields may be readily obtained.

In Region(II), the total transmitted field may be represented as

$$E_y^t(x, z) = \sum_{m=1}^{\infty} d_m \sin a_m(x+a) e^{-j\zeta_m z} \quad (2.1)$$

where

$$a_m = m\pi / (2a)$$

$$\zeta_m = \sqrt{k^2 - a_m^2}$$

To determine unknown coefficient  $d_m$ , it is necessary to match the boundary conditions of tangential E- and H-field continuities. First, the tangential E-field continuity along the  $x$ -axis ( $-\infty < x < \infty, z=0$ ) yields

$$\begin{aligned} E_y^s(x, 0) &= E_y^t(x, 0) & |x| < a \\ &= 0 & |x| > a \end{aligned}$$

Taking the Fourier transform on the both sides of above equation, we get

$$\bar{E}_y^s(\zeta) = \int_{-\infty}^{\infty} E_y^s(x, 0) e^{j\zeta x} dx = \int_{-a}^a E_y^t(x, 0) e^{j\zeta x} dx \quad (2.2)$$

Substituting (2.1) into (2.2), and performing integration with respect to  $x$ , we obtain

$$\bar{E}_y^s(\zeta) = \sum_{m=1}^{\infty} d_m \frac{a_m}{(\zeta^2 - a_m^2)} [e^{j\zeta a} (-1)^m - e^{-j\zeta a}] \quad (2.3)$$

Second, the tangential H-field continuity along  $-a < x < a, z=0$ , gives

$$\begin{aligned} H_x^i(x, 0) + H_x^r(x, 0) + H_x^s(x, 0) &= H_x^t(x, 0) \\ 2k_0 e^{jk_x x} - \int_{-\infty}^{\infty} \frac{k_1}{2\pi} \bar{E}_y^s(\zeta) e^{-j\zeta x} d\zeta \\ &= \sum_{m=1}^{\infty} d_m \zeta_m \sin a_m(x+a) \end{aligned} \quad (2.4)$$

Substituting (2.3) into (2.4), we obtain

$$2k_1 e^{jk_1 x} - \frac{1}{2\pi} \sum_{m=1}^{\infty} d_m a_m \int_{-\alpha}^{\infty} \frac{(-1)^m e^{jka} - e^{-jka}}{\zeta^2 - a_m^2} k_1 e^{-j\zeta x} d\zeta = \sum_{m=1}^{\infty} d_m \zeta_m \sin a_m (x+a)$$

In order to determine the coefficient  $d_m$ , we multiply the above equation by  $\sin a_m (x+a)$  and integrate the both sides with respect to  $x$  from  $-a$  to  $a$ , then we obtain

$$\frac{2k_1 a_n}{a_n^2 - k_1^2} [-(-1)^n e^{jk_1 a} + e^{-jk_1 a}] = \frac{1}{2\pi} \sum_{m=1}^{\infty} d_m I_{1mn} + d_n \zeta_n a \quad (2.5)$$

where

$$I_{1mn} = \int_{-\infty}^{\infty} \frac{a_n a_m [(-1)^m e^{jka} - e^{-jka}] [(-1)^n e^{-jka} - e^{jka}] k_1}{(\zeta^2 - a_m^2)(\zeta^2 - a_n^2)} d\zeta$$

The analytic contour integral evaluation of  $I_{1mn}$  may be performed in the complex  $\zeta$  plane to give

$$I_{1mn} = 2\pi a \eta_m \delta_{mn} - (I_{1nm} + I_{2nm}) \quad (2.6)$$

where  $\eta_m = \sqrt{k_0^2 - a_m^2}$ , and  $\delta_{mn}$  is the Kronecker delta. The explicit expressions for  $I_{1nm}$ ,  $I_{2nm}$  are given in [5] such as :

$$I_{1nm} = \int_0^{\infty} \frac{-4j\alpha\beta(-1)^n e^{2jk_0 a v} e^{-2jk_0 a v} \sqrt{v(-2j+v)}}{[(1+jv)^2 - \alpha^2][(1+jv)^2 - \beta^2]} dv \quad (2.7)$$

$$I_{2nm} = \int_0^{\infty} \frac{4j\alpha\beta \sqrt{v(-2j+v)}}{[(1+jv)^2 - \alpha^2][(1+jv)^2 - \beta^2]} dv$$

where  $\alpha = a_m / k_0$ ,  $\beta = a_n / k_0$

Performing integrations with respect to  $v$  [5], we obtain

$$I_{1mn} = -\frac{2\alpha\beta e^{2jk_0 a} (-1)^n}{(\alpha^2 - \beta^2)} \sum_{l=1}^{\infty} S_l [A(t_1) - A(t_2)] / \alpha - [A(t_3) - A(t_4)] / \beta \quad (2.8)$$

$$I_{2mn} = \frac{4j\alpha\beta}{(\alpha^2 - \beta^2)} \left[ \frac{\sqrt{1-\alpha^2}}{\alpha} \sin^{-1} \alpha - \frac{\sqrt{1-\beta^2}}{\beta} \sin^{-1} \beta \right]$$

where

$$S_l = \binom{n-1}{l-1} (0.5j)^{l-1}$$

$$A(t) = (-1)^l \pi^{l-0.5} e^n \operatorname{erfc}(\sqrt{pt}) + 2^{l-1} \sqrt{\pi} p^{0.5-l} \sum_{r=0}^{l-1} (2l-2r-3)!! (-2pt)^r$$

$$p = 2k_0 a$$

$\operatorname{erfc}(\dots)$ : complementary error function

$$t_1 = (\alpha-1)j, t_2 = (-\alpha-1)j, t_3 = (\beta-1)j,$$

$$t_4 = (-\beta-1)j$$

Note that  $I_{1mn}$  of (2.8) is expressed in terms of the asymptotic series of which  $l^{\text{th}}$  term has an order of  $O(1/k_0 a)^{l-0.5}$ . The series expression for  $I_{1mn}$  converges only for  $|2k_0 a / (m\pi)| > 1$ ; hence, it is computationally more efficient to use a fast-convergent integral (2.7) than (2.8) for the evaluation of  $I_{1mn}$ . When  $k_0 a \rightarrow \infty$ , the branch-cut contribution becomes negligible, thus  $I_{1mn} \rightarrow 2\pi a \eta_m \delta_{mn}$ .

Substituting  $I_{mn}$  of (2.6) into (2-5) and solving for  $d_m$ , we obtain :

$$D = (U - R)^{-1} S = S + RS + R^2 S + \dots \quad (2.9)$$

where  $D$  is the column matrix of elements  $d_m$ ,  $U$  the identity matrix,  $R$  the full matrix of elements  $r_{nm}$ , and  $S$  the column matrix of elements of  $s_n$ . The explicit expressions of  $r_{nm}$  and  $s_n$  are given as :

$$r_{nm} = \frac{(I_{1nm} + I_{2nm})}{2\pi(\xi_n + \eta_n)a}$$

$$s_n = \frac{2k_2 a_n [-(-1)^n e^{jk_2 a} + e^{-jk_2 a}]}{(\xi_n + \eta_n)a(a_n^2 - k_2^2)}$$

If  $k = k_0$ , then

$$r_{nm} = \frac{(I_{1mn} + I_{2mn})}{4\pi\xi_n a}$$

$$S_n = \frac{k_0 a_n [-(-1)^n e^{jk_0 a} + e^{-jk_0 a}]}{\xi_n a (a_n^2 - k_0^2)}$$

The examination of  $r_{nm}$  reveals that  $r_{nm} \sim O[1/\sqrt{k_0 a}]$  for  $k_0 a > 1$  and  $\xi_n + \eta_n \neq 0$ . For  $k_0 a \gg 1$ , the branch-cut contribution may be ignored ( $r_{nm} \approx 0$ ), thus (2.9) reduces to the Kirchhoff approximation such as

$$d_m \approx s_m \quad (2.10)$$

The branch-cut contribution  $I_{1mn}$  and  $I_{2mn}$  in  $I_{mn}$  account for coupling between  $E_y^s(x, z)$  of the continuous spectrum and  $E_y^t(x, z)$  of the discrete spectrum. When  $k_0 a \gg 1$ , the aperture magnetic current,  $E_y^t(x, 0)$ , is approximately given as  $E_y^t(x, 0)$  which has a very narrow spectral width; hence, the branch-cut contributions can be ignored.

Another special case of interest is low-frequency scattering ( $k_0 a < 1$ ). When  $k_0 a < 1$ , the most dominant element among  $r_{nm}$  is  $r_{11}$  whose value is approximately given by  $2/\pi^2$ . Hence, we have

$$d_1 \approx s_1 / (1 - r_{11}) \quad (2.11)$$

### III. Numerical Computations

The time-averaged power density  $P$ , which is received by the flanged parallel-plate waveguide, is

$$P = \frac{1}{2} \int_{-a}^a \text{Re}(\bar{E}^t \times \bar{H}^{t*}) \cdot (-\hat{z}) dx$$

$$= \frac{a}{2\omega\epsilon} \sum_{n=1}^{\infty} \text{Re}(\xi_n^*) |d_m|^2$$

where  $\bar{E}^t$  and  $\bar{H}^t$  are, respectively, the transmit-

ted electric and magnetic field vectors and the symbols  $\text{Re}(\dots)$  and  $(\dots)^*$ , respectively, denote the real part of  $(\dots)$  and the complex conjugation of  $(\dots)$ .

The far-zone scattered field at distance  $r$  from the origin can be evaluated by utilizing the stationary phase approximation such as

$$E_y^s(\theta_s, \theta) = e^{j(k_0 r - \pi/4)} \sqrt{\frac{k_0}{2\pi r}} \cos\theta_s \sum_{m=1}^{\infty} d_m a_m \frac{e^{-jk_0 a \sin\theta} (-1)^m - e^{jk_0 a \sin\theta}}{(k \sin\theta_s)^2 - a_m^2} \quad (3.12)$$

where  $\theta = \sin^{-1}(x/r)$  and  $r = \sqrt{x^2 + z^2}$

We first evaluate the scattered field for low-frequency scattering ( $k_0 a \ll 1$ ). Substituting (2.11) into (3.12), and taking the first leading term ( $m=1$ ), we obtain

$$E_y^s(\theta_s, \theta) \approx 0.5(k_0 a)^2 \frac{e^{j(k_0 r - 3\pi/4)}}{\sqrt{k_0 r}} \cos\theta \cos\theta_s \quad (3.13)$$

Note that (3.13) agrees with other low-frequency solution of scattering from a narrow groove [6].

In Table 1, the transmission coefficients  $d_m$  are tabulated versus  $2a/\lambda$  for  $\theta = 0^\circ$ . Note that  $d_2 = d_3 = \dots = 0$  because  $\theta = 0^\circ$ .

In Fig. 2,  $|d_m|$  are plotted versus  $\theta$  for  $k_0 a = 10$  ( $k = k_0$ ). In order to obtain the exact and approximate solutions, (2.9) and (2.10) are respectively used. Fig. 2 shows that the approximate solution (2.10) agrees well with the exact one (2.9) in high frequency scattering.

Fig. 3 show the scattering width  $\sigma$  ( $\theta^s = -\theta$ ) versus  $\theta$  for  $k_0 a = 10$  where  $\sigma = \lim_{r \rightarrow \infty} 2\pi r |E_y^s(\theta_s, \theta) / E_y^t(\theta)|^2$ . The number of coefficients  $d_m$  used in the computation is 10. The comparison of the exact solutions between two cases ( $k = k_0$  and  $\sqrt{3}k_0$ ) shows that an increase in  $k$  results in a decrease in  $\sigma$ . In Fig. 3, the exact solution is compared with the UTD solution which may be

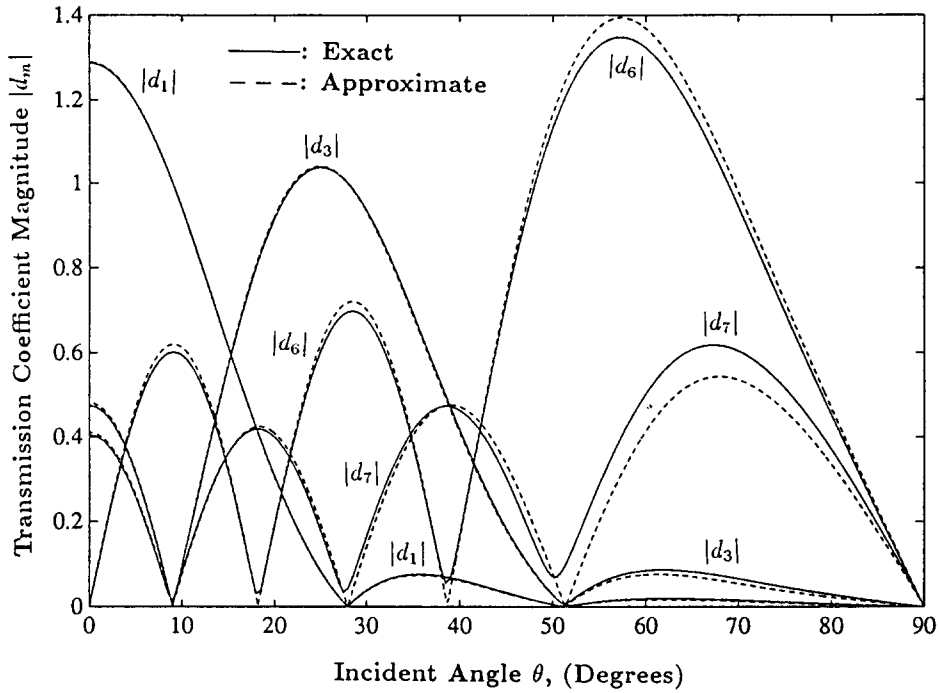


Fig. 2. Transmission Coefficient Magnitude  $|d_m|$  versus  $\theta$  for  $k_0 a = 10$  ( $k_0 = k$ )

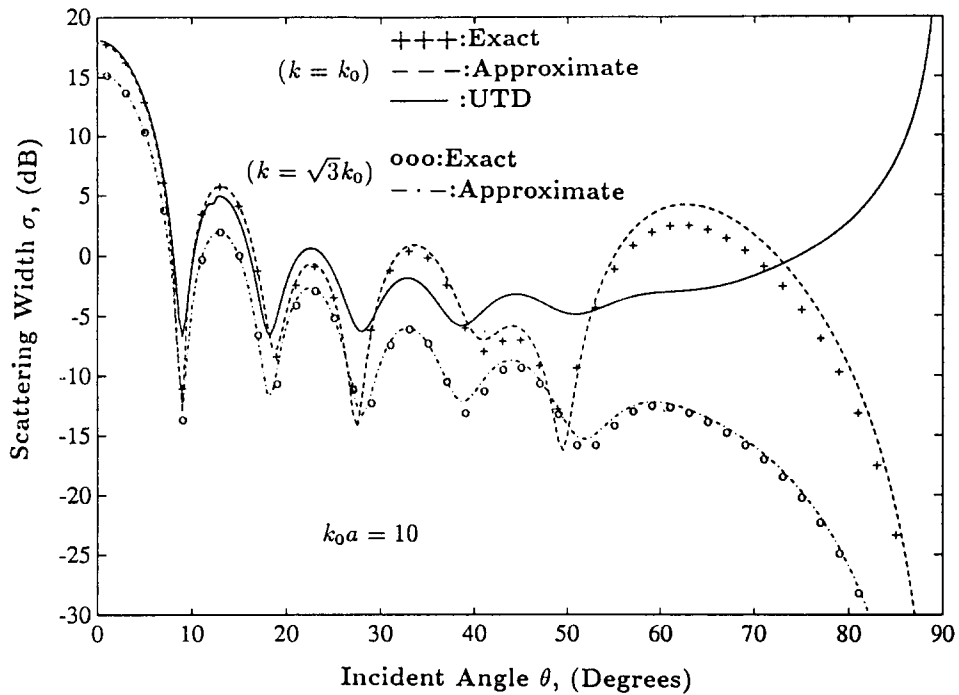


Fig. 3. Scattering Width  $\sigma$  ( $\theta_s = -\theta$ ) versus  $\theta$   $k_0 a = 10$ ,  
 ( $k = k_0$ , +++: exact, ---: approximate, —: UTD),  
 ( $k = \sqrt{3}k_0$ , ooo: exact, - - -: approximate)

Table 1. Transmission Coefficient  $d_m$  versus  $2a/\lambda$  for  $\theta = 0^\circ$  ( $k_0 = k$ )

$2a/\lambda$	Amplitude of $d_m$			Phase, degrees		
	$d_1$	$d_3$	$d_5$	$d_1$	$d_3$	$d_5$
0.51	3.0714	0.1710	0.0738	-19.61	-41.26	-37.79
0.61	2.0517	0.1506	0.0592	-7.27	-63.11	-55.66
0.71	1.7721	0.1771	0.0644	-3.26	-76.02	-68.30
0.81	1.6238	0.2210	0.0758	-1.27	-83.70	-76.61
0.91	1.5304	0.2833	0.0910	-0.20	-87.72	-81.45
1.01	1.4461	0.3635	0.1092	0.36	-89.03	-83.66
1.11	1.4194	0.4684	0.1299	0.61	-88.06	-83.80
1.21	1.3841	0.6088	0.1524	0.65	-84.83	-82.08
1.31	1.3565	0.8061	0.1754	0.53	-78.73	-78.34
1.41	1.3344	1.1150	0.1947	0.22	-67.75	-71.60
1.51	1.3262	1.5705	0.1600	-0.83	-27.14	-59.36
1.61	1.3327	1.0477	0.1595	-0.55	-12.05	-75.68

obtained by superimposing the singly-diffracted solution [2]. The comparison between the UTD solution and ours indicates a good agreement (less than 2dB error) when  $\theta < 20^\circ$ .

#### IV. Concluding Remarks

Using the Fourier transform and mode-matching approach, we obtain the series solution to scattering from the flanged waveguide. The numerical computations are performed to illustrate the behaviors of the fields scattered and received by the flanged-parallel plate waveguide. The series solution, which is based on (2.9), is exact and very efficient in the numerical computation.

#### References

1. A. Michaeli, "A new asymptotic high-frequency analysis of electromagnetic scattering by a pair of parallel wedge : Closed form results," Radio Science, vol.20, no. 6, pp.1537-1548, Nov.-Dec. 1985.
2. M. Schneider and R.J. Luebbers, "A general uniform double wedge diffraction coefficients," IEEE Trans. on Antennas and Propagat., no. 1, pp.8-14, Jan. 1991.
3. K. Hongo and Y. Ogawa, "Receiving characteristics of a flanged parallel plate waveguide," IEEE Trans. on Antennas and Propagat., pp. 424-425, Mar. 1977.
4. H.M. Nussenzveig, "Solution of diffraction problem, 1. The wide double wedge, 2. The narrow double wedge," Phil. Trans. Royal Soc. London, Ser. A, vol.252, pp.1-51.
5. H.J.Eom, T.J. Park, and K. Yoshitomi, "An analysis of TM scattering from a rectangular channel in a conducting plane," Submitted to the Journal of Applied Physics for publication.
6. K. Barkeshli and J.L. Volakis, "Scattering from narrow rectangular filled grooves," IEEE Trans. on Antennas and Propagat. vol. AP-39, no.6, pp.804-810, June 1991.